

Computer Simulation Comparison of Tripolar, Bipolar, and Spline Laplacian Electrocardiogram Estimators

T. Chen, W. Besio, *Senior Member, IEEE*, and W. Dai

Abstract—A comparison of the performance of the tripolar and bipolar concentric as well as spline Laplacian electrocardiograms (LECGs) and body surface Laplacian mappings (BSLMs) for localizing and imaging the cardiac electrical activation has been investigated based on computer simulation. In the simulation a simplified eccentric heart-torso sphere-cylinder homogeneous volume conductor model were developed. Multiple dipoles with different orientations were used to simulate the underlying cardiac electrical activities. Results show that the tripolar concentric ring electrodes produce the most accurate LECG and BSLM estimation among the three estimators with the best performance in spatial resolution.

I. INTRODUCTION

THE body surface Laplacian potential mapping (BSLM) using body surface Laplacian electrocardiogram (LECG) has been proven to provide more spatial details in differentiating multiple simultaneously active sources and source locating [1]-[7]. LECG was estimated using tripolar and bipolar concentric ring electrode LECG active sensors [1], [2], [8]-[10] and spline LECG estimator [4], [5]. Previous computer simulation and tank experiments [9] have demonstrated that tripolar LECG provides more detailed spatial information for the underlying source dipoles than bipolar LECG. Further computer simulation and modeling [6] showed tripolar BSLM has better spatial resolution in imaging spatially distributed cardiac electrical activity than bipolar BSLM. He et al. [4] and Li et al. [5] showed spline LECG had better performance than five-point method LECG, which is an estimate of bipolar LECG, with higher correlation coefficient as compared with the analytical LECG. It is of interest to compare all three LECG estimators to determine which has the best performance in specific circumstances.

II. METHODS

A. Simplified Heart-Torso Model

To compare the Laplacian estimators in a controlled environment a simplified human heart-torso model was

T. Chen was with Louisiana Tech University, Department of Biomedical Engineering (e-mail: tingwithers@yahoo.com).

W. Besio, is with the University of Rhode Island, Department of Electrical, Computer, and Biomedical Engineering, Kingston, RI 02881 USA, corresponding author (e-mail: besio@ele.uri.edu).

W. Dai is with the Mathematics and Statistics Department,, Louisiana Tech University, Ruston, LA USA, (e-mail: dai@coes.latech.edu).

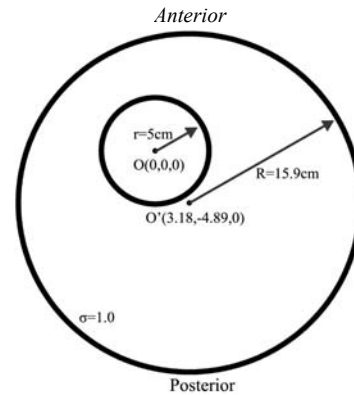


Fig. 1. Schematic of the heart-torso sphere-cylinder model. The inner and outer circles represent the epicardial and torso surface as seen from the top respectively. O and O' refer to the centers of the heart sphere and the torso cylinder. The height of the torso is 40 cm.

developed. Fig. 1 shows the model schematic as seen from the top. The model was approximated as a homogeneous conductor with a single normalized interior conductivity of 1.0 Sm^{-1} . The cylindrical surface of the torso was divided into a 2000 by 800 grid with a resolution of 0.05 cm.

B. Tripolar and Bipolar Concentric Ring Electrodes

Tripolar and bipolar concentric ring electrodes (Fig. 2) were modeled conforming to the curvilinear torso cylinder surface to calculate the body surface potential, tripolar, and bipolar LECG. The center disc, middle ring, and outer ring each covered 1, 92, 174 nodes respectively on the torso cylinder surface. The potential of each element was calculated by taking the average potential of all nodes within the inner and outer radii of each element as follows:

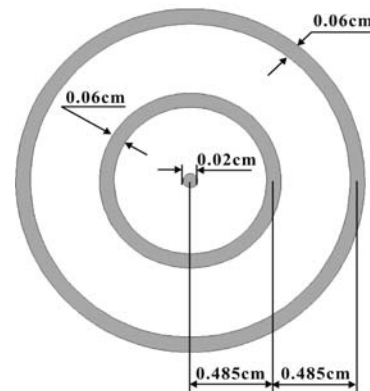


Fig. 2. Schematic of the tripolar and bipolar concentric ring electrode with a dia. of 2 cm. For bipolar, the middle ring is not used.

$$V_{element} = \frac{1}{M} \sum_{i=1}^M v_i \quad (1)$$

where $V_{element}$ represents the average potential of the center disc, middle ring or outer ring, M is the number of nodes that make up each element, and v_i is the potential at the i^{th} node. By activating different disc and ring elements the unipolar electrode, bipolar, and tripolar concentric ring electrodes were achieved. The spline, bipolar and tripolar LECG were calculated based on the equations presented in [1], [4], and [10].

Three topologies of arrays of $5 \times 5=25$, $9 \times 9=81$, and $11 \times 11=121$ concentric ring electrodes were employed to encompass the same anteriolateral area of the torso cylinder surface, achieving the spatial sampling rates of 5 cm, 2.5 cm, and 2 cm, respectively. The model of Fig. 3, developed using Matlab® 6.5, shows the three dimensional (3D) heart-torso model with 121 electrodes on the torso surface.

C. Source Dipole Models

Two kinds of source dipole directions were used to simulate the underlying cardiac electrical activities [1], [2]:

TABLE I
DIPOLE CONFIGURATIONS

Dipole config.	Dipole number and type	Position and Eccentricity within the heart	Separating angle between dipoles	Coordinates
^a C.1	1 ^b R	^d A 60%	n/a	(-1.5, 2.6, 0)
^a C.2	2 R	A 60%	60°	(±1.5, 2.6, 0)
^a C.3	2 ^c T	A 80%	20°	(±0.69, 3.94, 0)

^aC.1~C.3: dipole configurations 1~3, ^bR: radial dipole, ^cT: tangential dipole, ^dA: anterior.

(1) radial dipoles; and (2) tangential dipoles. By changing the number and location of source dipoles, various dipole configurations were simulated (Table I).

D. Noise Contamination

In this study two types of noise with different noise levels

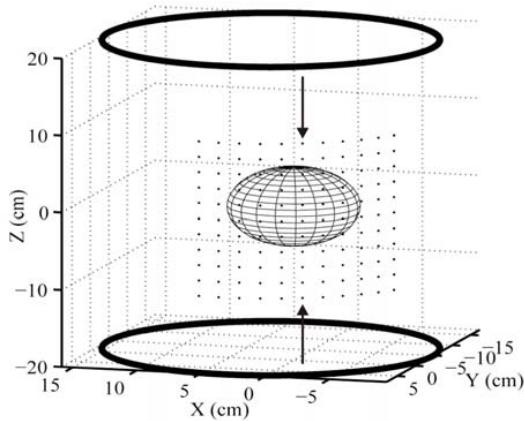


Fig. 3. 3D heart-torso model with $11 \times 11=121$ electrodes. The dots represent the centers of the electrodes. The two solid arrow lines indicate the central column.

were simulated: (1) Potential noise (PN) by activating potential noise dipoles; and (2) Gaussian white noise (GWN). The noise level is defined by Equation (2).

$$NoiseLevel = \frac{(q/4\pi\epsilon_0\epsilon_r)^2_{noise}}{(q/4\pi\epsilon_0\epsilon_r)^2_{source}} \quad (2)$$

where ϵ_0 and ϵ_r are permittivity of the free space and body volume, q is the dipole charge.

E. Multiple Sources Localization and Separation

For source localization two dipoles 5 cm from, and oriented perpendicular to, the torso cylinder surface, with separations of 2.2, 2.3, 2.4, and 2.5 cm were simulated. There were 121 recording electrodes and the separation coefficient (SC) [3] was used to quantify the localization.

F. Comparison Parameter

The accuracy of the three LECG estimators was evaluated by computing the root-mean square error (RMSE) between the normalized estimated and analytical LECG. The RMSE is calculated as follows:

$$RMSE = \sqrt{\frac{1}{N} \sum_{i=1}^N (L_{\epsilon,i} - L_{a,i})^2} \quad (3)$$

where N denotes the number of the recording sites and was set to 25, 81, and 121 for different recording arrays. $L_{\epsilon,i}$ and $L_{a,i}$ denote the normalized estimated (tripolar, bipolar, or spline) and analytical LECG at each recording site. In this study the normalized LECG was calculated by dividing the LECG at each recording site by the largest LECG among these recording sites. Smaller RMSEs, represent more accurate LECG estimations.

One way ANOVA analysis was performed with the one-tail paired two-sample t-Test for pairwise comparisons among the RMSE of the estimated LECG with different recording electrodes.

III. RESULTS

A. Effects of Number of Recording Electrodes

Table II shows the RMSE of the three LECG estimators corresponding to different dipole configurations and recording arrays. For each dipole configuration, the RMSE of the tripolar and bipolar LECG did not change significantly as the number of electrodes increased ($p=0.4313$ and $p=0.3366$ between 25 and 121 electrodes for tripolar and bipolar LECG respectively with all dipole configurations). However, for the spline LECG in general, the more electrodes, the lower the RMSE ($p=0.0133$ between 25 and 121 electrodes for spline LECG with all dipole configurations).

TABLE II
RMSE OF THE THREE LECG ESTIMATORS

Ele No.	25			81			121		
	T	B	S	T	B	S	T	B	S
C.1	2.3e-4	4.05e-4	1.87e-3	2.27e-4	3.82e-4	7.08e-4	2.01e-4	3.71e-4	4.04e-4
C.2	2.53e-4	4.83e-4	1.59e-3	2.38e-4	4.24e-4	6.53e-4	2.12e-4	4.08e-4	3.60e-4
C.3	4.14e-4	6.3e-4	4.47e-3	4.94e-4	5.40e-4	1.78e-3	4.66e-4	4.98e-4	9.94e-4

For all three dipole configurations and each electrode array, the tripolar LECG always showed the lowest RMSE. The bipolar LECG had lower RMSE compared with the spline LECG when 25, 81 or 121 electrodes were used for all dipole configurations except for C.2 with 121 electrodes. The RMSE of the tripolar LECG with 25 electrodes is significantly lower than that of the spline LECG with 121 electrodes for all dipole configurations ($p=0.0491$).

B. Effects of Noise Contamination

Fig. 4 and 5 show the RMSE of the three estimated LECG corresponding to C.1 with PN and GWN. For PN two noise dipoles were activated at $(-12.72, -4.89, 12)$ and $(-12.72, -4.89, 13)$. The noise level was from 0% to 25% using 121 electrodes. The abscissa represents the noise level from 0% to 25% which is shown from 0 to 0.25. The ordinate represents the RMSE of the three estimated LECG under different noise levels. The RMSE of the tripolar LECG are significantly smaller than those of the bipolar and spline LECG for all PN levels ($p=3.44e-14$ tripolar vs bipolar LECG, $p=7.52e-12$ tripolar vs spline). In Fig. 4 the RMSE of the tripolar LECG with 25% PN is lower than those of the bipolar and spline LECG without PN. Similarly in Fig. 5 the RMSE of the tripolar LECG are less than those of the bipolar and spline LECG of all GWN levels. The RMSE of the tripolar LECG with higher levels of GWN are comparable to those of the bipolar and spline LECG with

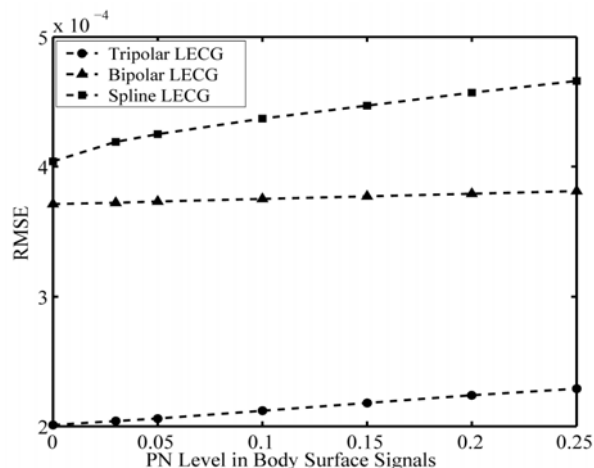


Fig. 4. RMSE of the tripolar (circle), bipolar (triangle) and spline (square) LECG for C.1 with two activated noise dipoles which were perpendicular to the torso surface. Noise level was from 0% to 25% and 121 electrodes were used.

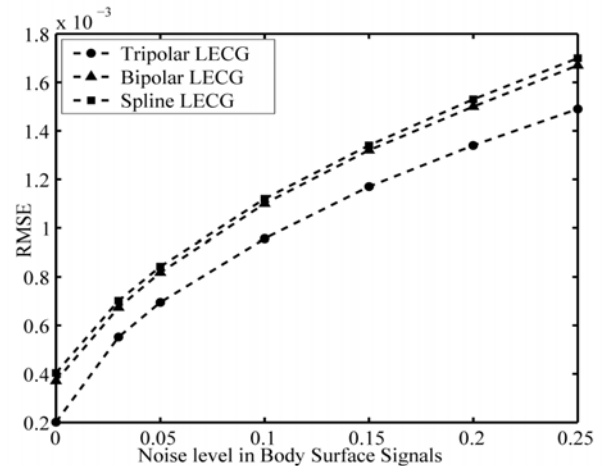


Fig. 5. RMSE of the tripolar (circle), bipolar (triangle) and spline (square) LECG for C.1 with GWN (1%~25%). 121 electrodes used.

lower levels of GWN. For example, in Fig. 5 the RMSE of the tripolar LECG with 20% or 25% GWN are lower than those of the bipolar and spline LECG with 15% or 20% GWN respectively.

C. Multiple Sources Localization and Separation

Fig. 6 shows the (a) tripolar, (b) bipolar, and (c) spline normalized estimated BSLMs and (d) shows the analytical BSLM with the separation distance of 2.3 cm. The black vertical dashed lines in each panel indicate the central column of the electrode array which is shown by the solid arrow lines on the torso cylinder surface in Fig. 3. The RMSE of the tripolar, bipolar, and spline BSLMs are $4.60e-$

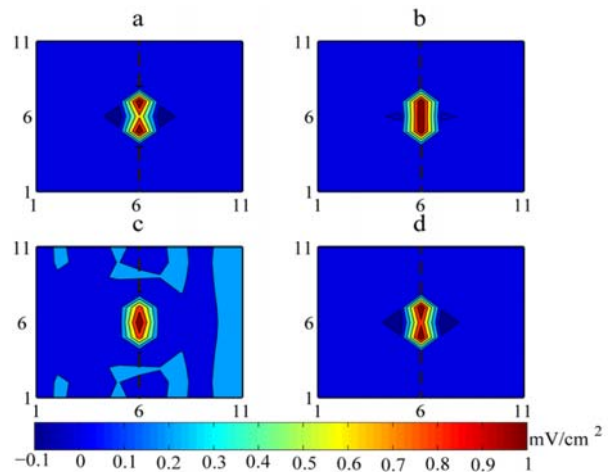


Fig. 6. Normalized estimated and analytical BSLM when the separation distance was 2.3 cm.

3, 4.84e-3, and 1.66e-2, respectively. In Fig. 6 only the tripolar BSLM shows the two maxima separately.

The SC values in Table III show the difference between the three estimated LECG. The higher the SC, the better the separation. When SC equals zero, the LECG can not differentiate two sources. In Table III, only the tripolar LECG SC was always positive representing that the tripolar LECG was capable of separating the two sources from the model. For the bipolar LECG, the SC was positive when the distance was greater than 2.3 cm. The spline LECG only showed positive SC when the distance was even larger (2.5 cm). Even when the three LECG estimates all had positive SC (2.5 cm apart), the tripolar LECG had the largest SC and the spline LECG the smallest. This demonstrates that the tripolar LECG provides the highest spatial resolution of the configurations tested.

TABLE III
SC OF THE ESTIMATED LECG WITH VARYING DIPOLE SEPARATION

	2.2 cm	2.3 cm	2.4 cm	2.5 cm
Tripolar LECG	0.0146	0.2151	0.3455	0.4319
Bipolar LECG	0	0	0.1079	0.2023
Spline LECG	0	0	0	0.0588

IV. DISCUSSION

Three LECG (tripolar, bipolar, and spline) estimators have been mainly used to approximate the body surface LECG and perform the BSLM. The local-based tripolar and bipolar LECG are obtained directly from the body surface. The global-based spline LECG is derived from the body surface potentials using the body surface geometric parameters which require further detail such as CT or MRI. The process of the interpolation may also introduce some error. To control experimental and biological conditions the present study performed the pattern comparison among three estimated LECG by building a simplified volume conductor model (eccentric sphere cylinder model) and simulating the cardiac electrical activities with radial or tangential dipoles.

The results show that the accuracy of spline LECG estimation compared to analytical LECG worsens significantly ($p=0.0133$ between 121 and 25 electrodes) when fewer electrodes are used. This is expected since spline interpolation depends on the spatial sampling rate. For the tripolar and bipolar LECG there is no significant change in accuracy while electrodes increased from 25 to 121 ($p=0.4313$ and $p=0.3366$ respectively). The tripolar LECG provides the most accurate LECG estimation among the three LECG estimators using fewer tripolar concentric ring electrodes (such as 25 or 81) without the knowledge of the body surface geometry parameters, unlike the spline LECG.

From Fig. 4 and 5, two findings are obvious. First, for all three LECG estimators, the higher the PN or GWN level, the

higher the RMSE. Second, the tripolar LECG always shows the least RMSE among the three estimated LECG for a given PN or GWN level. This reflects the global noise attenuation ability of the tripolar LECG. This improvement is not only shown at the same PN or GWN level, but it is also evident at higher noise levels when compared to the bipolar and spline LECG at lower noise levels. This is due to the common mode rejection ratio properties of the closely spaced tripolar electrode elements.

From Fig. 6, it can be seen that the abilities of localizing and separating the two sources are different for the three estimated LECG using concentric ring electrodes with diameter of 2 cm. The tripolar BSLM shows the best capability in distinguishing two concurrent cardiac activities with the highest SC and the spline BSLM provides the worst spatial resolution with the lowest SC (Table III).

In conclusion our results show that the high spatial resolution of the tripolar BSLM is appropriate for differentiating and locating two concurrent cardiac activities. The tripolar LECG and BSLM may enhance our capability and efficiency to image cardiac bioelectrical sources on the body surface. The current study used a simplified heart-torso model and simplified dipole configurations. Further analysis needs to be performed to determine if the same results hold for a more realistic volume conductor model with pacing sites. Future experimental and clinical studies in both normal subjects and cardiac diseased patients will be necessary to assess the tripolar LECG and BSLM in clinical diagnosis of disorders of the heart.

REFERENCES

- [1] B. He and R. Cohen, "Body surface Laplacian ECG mapping," *IEEE Trans. on BME* 39(11), pp. 1179-91, 1992.
- [2] B. He and R. Cohen, "Body surface Laplacian electrocardiographic mapping-A review," *Critical Reviews in BME* 23(5-6), pp. 475-510, 1995.
- [3] D. Wu, K. Ono, H. Hosaka and B. He, "Simulation of body surface Laplacian maps during ventricular pacing in a 3D inhomogeneous heart-torso model," *Methods Inf Med.*, pp. 39, 2000.
- [4] B. He, G. Li and J. Lian, "A spline Laplacian ECG estimator in a realistic geometry volume conductor," *IEEE Trans. on BME* 49, pp. 110-7, 2002.
- [5] G. Li, J. Lian, P. Salla, J. Cheng, P. Shah, I. Ramachandra, B. Avital and B. He, "Body surface Laplacian ECG mapping of ventricular epolarization in normal subjects," *J. Cardiovascular Electrophysiology* 14(1), pp. 6-27, 2003.
- [6] V. Soundararajan and W. Besio, "Simulated comparison of disc and concentric electrode maps during atrial arrhythmias," *IJBEM* 7(1), pp. 217-20, 2005.
- [7] D. Wei, "Laplacian electrocardiograms simulated using realistically shaped heart-torso model during normal and abnormal ventricular depolarization," *Electromagnetics* 21, pp. 593-605, 2001.
- [8] W. Besio, C. Lu and P. Tarjan, "A feasibility study for body surface cardiac propagation maps of humans from Laplacian moments of activation," *Electromagnetics* 21, pp. 621-32, 2001.
- [9] W. Besio, R. Aakula, K. Koka and W. Dai, "Development of a tri-polar concentric ring electrode for acquiring accurate Laplacian body surface potentials," *Annals of BME* 34(3), pp. 426-35, 2006.
- [10] W. Besio and T. Chen, "Tripolar Laplacian electrocardiogram and moment of activation isochronal mapping," *Physiol. Meas.* 28, pp. 515-529, 2007.